Chemical Physics Letters 478 (2009) 1–10

Contents lists available at ScienceDirect

Chemical Physics Letters

journal homepage: www.elsevier.com/locate/cplett

FRONTIERS ARTICLE

Quantum Monte Carlo for atoms, molecules and solids

William A. Lester Jr. [a,b,*], Lubos Mitas [c], Brian Hammond [d]

[a] Kenneth S. Pitzer Center, Department of Chemistry, University of California, Berkeley, CA 94720-1460, United States
[b] Chemical Sciences Division, Lawrence Berkeley National Laboratory, Berkeley, CA 94720, United States
[c] Department of Physics and Center for High Performance Simulation, North Carolina State University, Raleigh, NC 27695, United States
[d] Microsoft Corporation, 45 Liberty Boulevard, Great Valley Corp Ctr., Malvern, PA 19355, United States

ARTICLE INFO

Article history:
Received 28 June 2009
In final form 30 June 2009
Available online 3 July 2009

ABSTRACT

The quantum Monte Carlo (QMC) method has become increasingly important for solution of the stationary Schrödinger equation for atoms, molecules and solids. The method has been shown to exhibit high accuracy that scales better with system size than other *ab initio* methods. Moreover, as typically implemented, QMC takes full advantage of parallel computing systems. These attributes for electronic structure calculations will be described, as well as recent applications that demonstrate the breadth of the QMC approach.

1. Introduction

In the past decade, the field of computational science, the ability to simulate physical processes based on fundamental physical laws, has undergone rapid growth. This progress has been achieved not only due to the exponential increase in computing power now available, but also because of a new generation of simulation algorithms. However, each new generation of high-performance computing platforms presents a renewed challenge to the developers of computational methods to take full advantage of the underlying computer architecture. In many cases, the original computational method has not been well suited to both reduce the time to solution for a given physical system and, more importantly, to increase the accuracy of the simulation.

The *ab initio* simulation of the electronic structure of atoms, molecules, and solids has greatly benefited from an enormous increase in computing power, but it has also remained bound for the most part by approximations originally created to make the computations possible. The most popular of these approximations are those based on basis set expansions that have their origin with either the Hartree–Fock (HF) or Density Functional Theory (DFT) formalisms. These methods have presented a number of challenges to the use of massively parallel computers in addition to well-known limitations in their accuracy.

An alternate approach that shows great promise both in its inherent accuracy as well as its ability to make efficient use of modern computing power is quantum Monte Carlo (QMC). QMC is a broad term that can refer to a number of techniques that use stochastic methods to simulate quantum systems. For electronic structure theory, we are referring to the simulation of the electronic Schrödinger equation by the use of random numbers to sample the electronic wave function and its properties. QMC has consistently shown the ability to recover 90–95% of the electron correlation energy (the difference between the HF and exact energies), even in cases that are poorly described by the HF method, and for large systems with hundreds of electrons. For few-electron systems, the method is capable of solving the stationary Schrödinger problem exactly with minimal statistical error. A number of reviews of these topics have appeared recently [1–4].

Until recently, the success of the QMC method was limited to simulation and prediction of properties of small molecules consisting of light atoms, owing to the relatively large amount of computation required to reduce statistical error to physically significant levels. Great strides in algorithms combined with QMC's inherent parallelism have removed these limits and made possible the accurate simulation of much larger molecules, as well as solids. Advances in the method have widened the application of QMC to other electronic properties of these systems besides the energy. One of the greatest strengths of the approach is in the ability to numerically sample quantum operators and wave functions that cannot be analytically integrated or represented. This capability has enabled the QMC method to make significant contributions to fundamental understanding of the electronic wave function and its properties.

Interest has grown in the use of the QMC method for the study of a wide range of physical systems, including atomic, molecular, condensed-matter, and nuclear. In this Letter, we shall not address the latter area [5], which is mentioned only to indicate the broad range of phenomena accessible by the method. The general applicability of QMC has led us to limit consideration in this article to the electronic structure of the aforementioned systems due to space limitations and author interest. Path integral MC [6] will

* Corresponding author. Address: Kenneth S. Pitzer Center, Department of Chemistry, University of California, Berkeley, CA 94720-1460, United States.
E-mail address: walester@lbl.gov (W.A. Lester Jr.).

0009-2614/$ - see front matter © 2009 Elsevier B.V. All rights reserved.
doi:10.1016/j.cplett.2009.06.095

not be discussed, nor shall approaches for the determination of the internal energy of molecular systems, including clusters [7].

Certain properties make QMC particularly attractive for the treatment of electronic structure. These include limited dependence on basis set, unlike all other *ab initio* methods, high accuracy of energy calculations that are typically as accurate as other state-of-the-art ab initio methods [8], and weak dependence of computation on system size or scaling [9–11], as well as the ease of adaptation of QMC computer programs to parallel computers [12].

This Letter is organized as follows. Section 2 summarizes the main variants of QMC applied to atoms, molecules, and solids. These methods are variational Monte Carlo (VMC) and diffusion Monte Carlo (DMC). Section 2 also includes other issues that play an important role in the development of QMC. Section 3 briefly summarizes selected applications that provide an indication of the breadth and level of accuracy for systems studied to date. Finally, Section 3.2 briefly summarizes key points of the Letter.

2. QMC methods

The QMC methods to be discussed solve the non-relativistic, time-independent, electronic Schrödinger equation,

$$\mathscr{H}\Phi = E\Phi, \tag{1}$$

where $\mathscr{H}$ is the molecular Hamiltonian. The Hamiltonian contains the kinetic and potential energy operators for the electrons, $\mathscr{H} = \mathscr{J} + \mathscr{V}$, where $\mathscr{J}$ is the Laplacian operator for the kinetic energy,

$$\mathscr{J} = -\frac{1}{2}\nabla^2, \tag{2}$$

(∇^2 is the sum of the kinetic energy operators, $\sum\left(\frac{d^2}{dx_i^2}+\frac{d^2}{dy_i^2}+\frac{d^2}{dz_i^2}\right)$ for each electron, i) and $\mathscr{V}$ is the potential energy operator that for a system comprised of N_e electrons and N_n nuclei with nuclear charges Z_A and no external fields is,

$$\mathscr{V} = -\sum_{i=1}^{N_e}\sum_{A=1}^{N_n}\frac{Z_A}{r_{iA}} + \sum_{i=1}^{N_e}\sum_{j>i}^{N_e}\frac{1}{r_{ij}} + \sum_{A=1}^{N_n}\sum_{B>A}^{N_n}\frac{Z_A Z_B}{r_{AB}}, \tag{3}$$

where r is the distance between particles. Atomic units have been used, in which the mass and the charge of the electron are set to unity.

To solve Eq. (1) using Monte Carlo, we start with the time-dependent Schrödinger equation written in *imaginary time* by substituting $\tau = it$,

$$-\frac{\partial\phi(\mathbf{X},\tau)}{\partial\tau} = \mathscr{J}\phi(\mathbf{X},\tau) + (\mathscr{V} - E_T)\phi(\mathbf{X},\tau), \tag{4}$$

that has the formal solution

$$\phi(\mathbf{X},\tau) = \sum_{k=0}^{\infty} C_k \Phi_k(\mathbf{X}) e^{-(E_k - E_T)\tau}, \tag{5}$$

where $\phi(\mathbf{X},\tau)$ is the time dependent wave function and $\Phi_k(\mathbf{X})$ are the time independent eigenstates of the Schrödinger equation. The quantity E_T is an energy offset chosen to reduce the impact of the exponential factor. As $\tau \to \infty$, Eq. (5) converges exponentially to the lowest electronic state with non-zero C_k, which is usually the ground state Φ_0. Eq. (4) has been written with the Hamiltonian expanded to show that it has the form of a diffusion equation (the kinetic energy term) and a rate equation (with 'rate constant' $\mathscr{V} - E_T$). Both these processes can be simulated using Monte Carlo sampling methods to propagate the solution to large imaginary time. (Note: since τ is imaginary time, no description of real time dynamics is intended; see, however, Grossman and Mitas [13]).

The simulation is performed by constructing an initial ensemble of walkers, each of which represents the positions of all the electrons in the system: $\mathbf{R} = \{x_1, x_2, \ldots, x_n\}$. Each of these electronic configurations then undergoes a random walk in imaginary time until sufficient time has elapsed for the excited states to decay away. The resulting density distribution is proportional to Φ_0. Such a simulation, however, poses two serious problems. First, to simulate a diffusion equation, one requires the distribution to represent a positive density, whereas for Fermion systems, Φ_0 necessarily changes sign. Second, the rate equation depends on the potential energy which varies widely and diverges when two particles approach, which will cause the Monte Carlo simulation to be unstable.

Both these issues can be dealt with by the introduction of *importance sampling*. Choose a *trial* function, Ψ_T that is a good approximation to the desired state Φ_0. Define a new function, $f(\mathbf{X},\tau) \equiv \Psi_T\phi(\mathbf{X},\tau)$, and then rewrite the imaginary-time-dependent Schrödinger equation in terms of this new function:

$$-\frac{\partial f(\mathbf{X},\tau)}{\partial\tau} = -\frac{1}{2}\nabla^2 f(\mathbf{X},\tau) + \nabla\cdot(\mathbf{F}_Q(\mathbf{X})f(\mathbf{X},\tau)) + (E_L(\mathbf{X}) - E_T)f(\mathbf{X},\tau), \tag{6}$$

where $\mathbf{F}_Q = \Psi_T^{-1}\nabla\Psi_\tau$, and $E_L = \Psi_\tau^{-1}\mathscr{H}\Psi_T$. The quantity $\mathbf{F}_Q$ is a vector field pointing towards regions of large Ψ_T, and E_L is the local energy of Ψ_T. The effect of importance sampling is twofold: first, it introduces the term $\nabla\cdot(\mathbf{F}_Q(\mathbf{X})f(\mathbf{X},\tau))$, which is a directed drift moving the system to areas of large Ψ_T, and second, the rate term now depends on the local energy, which is much smoother than $\mathscr{V}$ for good trial function choices. It can be seen from the form of the local energy, as $\Psi_T \to \Phi, E_L$ becomes the constant, E_0, the ground state energy.

Once $f(\mathbf{X},\tau)$ has converged to $\Psi_T\Phi_0$, expectation values with respect to Φ_0 may be measured by continuing the Monte Carlo simulation and sampling various operators, the most important of which is the Hamiltonian. The energy of Φ_0 is obtained from the local energy as follows,

$$\begin{aligned}\langle E_L\rangle &= \int \Psi_T\Phi_0\frac{\mathscr{H}\Psi_T}{\Psi_T}d\mathbf{x}\Big/\int \Psi_T\Phi_0 d\mathbf{x}\\ &= \int \Psi_T\mathscr{H}\Phi_0 d\mathbf{x}\Big/\int \Psi_T\Phi_0 d\mathbf{x} = E_0.\end{aligned} \tag{7}$$

The last step is obtained from the Hermitian property of $\mathscr{H}$. One difficulty imposed by importance sampling is that all properties involving an operator $\mathscr{A}$ that does not commute with the Hamiltonian will result in a mixed estimate, $\langle\Psi_T \mid \mathscr{A}\mid\Phi_0\rangle$ rather than the 'pure' estimate $\langle\Phi_0 \mid \mathscr{A}\mid\Phi_0\rangle$. There are several methods to extract the pure Φ_0^2 distribution needed for operators that do not commute with the Hamiltonian, but we shall not describe them here.

Simulating the importance-sampled Schrödinger equation is formally the same as above, except that the diffusion process now has a directed drift, and a new 'rate constant' given by $E_L - E_T$. The sampling procedure can be performed in a number of ways. Below, we present the two QMC approaches that dominate current interest and have been used for most calculations: *Variational Monte Carlo* (VMC) and *Diffusion Monte Carlo*(DMC). VMC is a method that samples from the Ψ_T^2 distribution, yielding the energy and other properties of the trial function. DMC is a projector method that samples from the mixed $\Psi_T\Phi_0$ distribution and, in principle, can yield exact energies and properties.

2.1. VMC

The VMC method [14] exploits the QMC formalism above to evaluate the expectation values of a known trial function, Ψ_T, rather than the ground state Φ_0. This capability is useful when the function Ψ_T cannot be integrated analytically or by other numerical methods, and is the method is especially valuable for

investigating novel wave function forms. VMC is also used as a precursor to DMC as a method to optimize Ψ_T and to generate initial walker distributions.

If the local-energy dependent term in the importance-sampled Schrödinger equation is removed, the resulting equation will converge to the solution $f = \Psi_T^2$ rather than $\Psi_T\phi$,

$$-\frac{\partial f(\mathbf{X},\tau)}{\partial \tau} = -\frac{1}{2}\nabla^2 f(\mathbf{X},\tau) + \nabla\cdot(\mathbf{F}_Q(\mathbf{X})f(\mathbf{X},\tau). \tag{8}$$

One can generate an ensemble of pseudo particles $\{\mathbf{R}_i\}$ via the related Langevin equation, that can be integrated over a small time step $\delta\tau$, to give a prescription for moving a pseudo particle with coordinates $\mathbf{R}$ to a new position $\mathbf{R}'$,

$$\mathbf{R}' = \mathbf{R} + D\mathbf{F}_Q(\mathbf{R})\delta\tau + \chi. \tag{9}$$

Here D is the diffusion constant (1/2) and χ is a Gaussian random variable with zero mean and variance $2D\delta\tau$. Once the ensemble has converged to the distribution Ψ_T^2, properties such as the local energy can be sampled. In practice, Metropolis sampling is introduced to further speed convergence and to eliminate any dependence on the time step. Trial functions for VMC can be constructed in a variety of ways typically guided by suitability to the system under consideration.

2.2. DMC

There are two primary difficulties to be overcome to simulate the particles, i.e., the electrons in imaginary time. These are: how to create a stochastic process that generates the proper distribution, and how to obtain the appropriate Fermion ground state, not the lowest energy solution which would be the Boson ground state.

The DMC method is a projector approach in which a stochastic imaginary-time evolution is used to improve a starting trial wave function. The governing equations can readily be obtained by multiplying the time-dependent Schrödinger equation in imaginary time, Eq. (4), by a known approximate wave function Ψ_T. One defines a new distribution f given as the product of Ψ_T and the unknown exact wave function Φ. The resulting equation in terms of f has the form of a diffusion equation with drift, provided f is positive definite. In general, the exact Φ and the approximate Ψ_T will differ in various regions so that their product will not be positive unless one imposes the fixed-node boundary condition, namely, that $f \geqq 0$. The wave function f is an approximation to Φ_0 in that the nodes of f are the same as Ψ_T.

2.2.1. The short time approximation to Green's function

In order to create an ensemble of walkers evolving in imaginary time with the distribution f, one needs a method similar to that of VMC that moves the particles of the system through a series of time steps. This aim can be achieved in a manner similar to VMC, by integrating the Schrödinger equation to obtain f at time $\tau + \delta\tau$ from f at time τ,

$$f(\mathbf{R}',\tau+\delta\tau) = \int G(\mathbf{R}'\leftarrow\mathbf{R},\delta\tau)f(\mathbf{R},\tau)d\mathbf{R}. \tag{10}$$

The function $G(\mathbf{R}'\leftarrow\mathbf{R},\delta\tau)$ is Green's function of the Hamiltonian, formally related by $G = e^{-\mathscr{H}\delta\tau}$. The exact Green's function is a solution to the Schrödinger equation, and is therefore unknown, in general. However, one can approximate Green's function as $G = e^{-\delta\tau\mathscr{V}/2}e^{-\delta\tau\mathscr{J}}e^{-\delta\tau\mathscr{V}/2}$ which is only exact in the limit that $\delta\tau\to 0$ since $\mathscr{J}$ and $\mathscr{V}$ do not commute. For the importance sampled equation, Eq. (6), the kinetic energy term is modified to include the drift term, so that the expression for the short-time approximation to Green's function is

$$G(\mathbf{R}'\leftarrow\mathbf{R},\delta\tau) = (4\pi D\delta\tau)^{-3N_e/2}e^{-[\mathbf{R}'-\mathbf{R}-\delta\tau D\mathbf{F}_Q(\mathbf{R})]^2/(2D\delta\tau)}e^{-\delta\tau[E_L(\mathbf{R}')-E_L(\mathbf{R})-2E_T]/2}. \tag{11}$$

Green's function is now composed of a Gaussian probability distribution function with a mean that drifts with velocity $D\mathbf{F}_Q$ and spreads with time as $\sqrt{\delta\tau}$, and a rate term that grows or shrinks depending on the value of local energy relative to E_T. Hence this Green's function has the expected behavior of a diffusion-like term multiplied by a branching term.

2.2.2. The DMC walk

There are numerous methods to carry out the simulation (as well as other possible short-time approximations), but one of the simplest methods is as follows:

(a) Create an initial ensemble of walkers, $f(\mathbf{R},0)$, typically the result of a VMC simulation.
(b) For each walker, each electron (with coordinates $\mathbf{r}_i$) will diffuse and drift one at a time for a time step $\delta\tau$ by,

$$\mathbf{r}_i' = \mathbf{r}_i + D\delta\tau\mathbf{F}_Q(\mathbf{r}_i) + \chi, \tag{12}$$

where χ is a pseudo random number distributed according to the Gaussian part of $G(\mathbf{R}'\leftarrow\mathbf{R},\delta\tau)$.
(c) If the electron move crosses a node of the trial function the move is rejected, then go back to (b) for the next electron.
(d) To insure detailed balance, accept the move of the electron with probability $A(\mathbf{R}'\leftarrow\mathbf{R}) \equiv \min(1, W(\mathbf{R}'\leftarrow\mathbf{R}))$, where

$$W(\mathbf{R}'\leftarrow\mathbf{R}) \equiv \frac{|\Psi_T(\mathbf{R}')|^2 G(\mathbf{R}'\leftarrow\mathbf{R},\delta\tau)}{|\Psi_T(\mathbf{R}')|^2 G(\mathbf{R}\leftarrow\mathbf{R}',\delta\tau)}. \tag{13}$$

(e) Return to step (b), moving all the electrons in this walker. Compute the local energy and other quantities of interest.
(f) Calculate the multiplicity M (the branching probability) for this walker from the rate term in Green's function,

$$M = \exp\left(-\delta\tau_a\{[E_L(\mathbf{R}')+E_L(\mathbf{r})]/2 - E_T\}\right). \tag{14}$$

The quantity $\delta\tau_a$ is the effective time step of the move, taking into account the rejection of some moves. The effective time of the move is calculated from the mean-squared move distance that is $\langle r_{total}^2\rangle = 6D\delta\tau$ without rejection. With rejection, the move distance is $\langle r_a^2\rangle = 6D\delta\tau_a$ where

$$\delta\tau_a = \frac{\langle r_a^2\rangle}{\langle r_{total}^2\rangle}. \tag{15}$$

The walker is then replicated or destroyed based on M. To do so, create the integer $\overline{M} = \mathrm{int}(M+\xi)$ where ξ is a random number between zero and one. If $\overline{M} \geqslant 1$, then make $\overline{M}$ copies, otherwise the multiplicity is zero and the walker is removed from the ensemble. (In some implementations, the ratio $M/\overline{M}$ is kept as a weight for the walker. In the pure DMC method, M is kept as a weight and the ensemble size remains fixed.)
(g) Weight the local energy and other quantities of interest by M.
(h) Return to step (b) for the remaining walkers.
(i) Compute the ensemble averages and continue to the next time step. At suitable intervals one can update the trial energy E_T to regulate the size of the ensemble. It may also be necessary to 'renormalize' the ensemble when it grows too large or too small, which can be achieved by randomly deleting or replicating walkers. Care must be taken as renormalization can introduce an energy bias.
(j) At the end of the run the final energy and properties are computed and various statistical methods can be applied to determine the variance of the mean values. As an indicator of the energy as a function of simulation time, see Fig. 1.

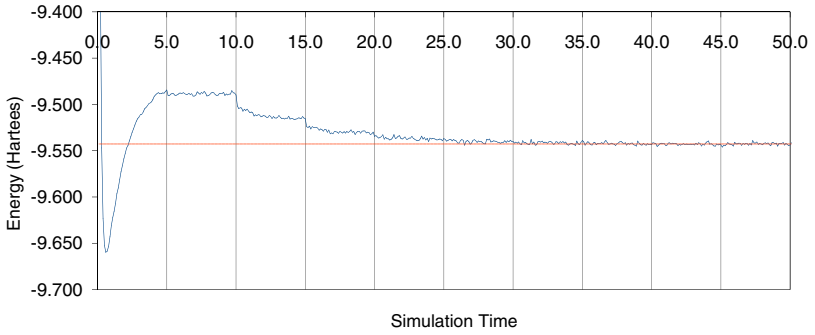

Fig. 1. This plot traces the average energy over simulation time for a VMC calculation of the electronic energy of nitrogen atom using effective core potentials. Each point corresponds to an average over 1.0×10^6 walkers. Initial electron coordinates were sampled from a spherically symmetric distribution around the nucleus. From $t = 0$ to $t \sim 4$, the walkers drift to their equilibrium distribution, Ψ_T^2. Before reaching equilibrium, the energy average has no relation to the energy of the wavefunction. Convergence of the optimization procedure is reached after about six iterations.At this point, the wavefunction parameters and the walker distribution have converged, but the energy continues to fluctuate around the final value due to instantaneous random errors.The anti-symmetric wavefunction used here was determined from a restricted open-shell Hartree–Fock calculation using the 6-31G basis set and the soft effective core potential from Ovcharenko et al. [15]. A nine-term Boys–Handy expansion [16,17] was used for the correlation function. Only the linear coefficients of the terms in the expansion were optimized, with selected parameters held fixed to satisfy the electron–electron cusp condition. The use of soft ECPs eliminates the electron–nucleus cusp condition.

(k) Repeat for several values of $\delta\tau$. Because the simulation is only exact in the limit $\delta\tau \to 0$ it is necessary to either extrapolate to zero time or demonstrate that the bias is smaller than the statistical uncertainty of the result.

2.2.3. The variational principle in DMC

The DMC method is fundamentally a ground state method. No bounds exist for excited states similar to the variational principle for ground states. Nevertheless, excited states that are the lowest of a given symmetry are routinely addressed [18], and it has been shown that excited states of the same symmetry as a lower state can be computed with the fixed node method with excellent results [19].

2.3. Trial wave functions

2.3.1. Form of the trial function

The types of wave functions that have been used in VMC and DMC begin with those of basis set quantum chemistry, referring primarily to HF and various multi-configuration formalisms. The latter include multi-configuration self-consistent-field (MCSCF) and configuration interaction (CI). In addition, various density functional theory (DFT) wave functions have been used, in particular, a number of generalized gradient forms [20]. There has been some use of Moeller–Plesset perturbation theory functions, but state-of-the-art coupled cluster forms have not been used as trial wave functions owing to the difficulty in constructing wave functions in the approach.

Trial wave functions play two important roles in QMC calculations. The first is to avoid the fermion sign problem by use of the fixed-node approximation. The second is efficiency: statistical fluctuations are significantly reduced by increasing trial function accuracy. This is practically very important since the efficiency gain can reach two to three orders of magnitude. For cutting-edge applications that involve large numbers of electrons or high statistical accuracy, trial function quality is crucial and can determine whether computations are feasible.

To satisfy both these requirements, trial functions are typically chosen to have the following general form [1–4]:

$$\Psi(\mathbf{R}) = \Psi_A(\mathbf{R}) e^{U_{corr}}, \tag{16}$$

where $\Psi_A(\mathbf{R})$ is an antisymmetric wave function and the second term is a symmetric factor that depends explicitly on interparticle coordinates. Focusing first on the correlation function one can expand U_{corr} in functions of two, three, and higher-order particle interactions,

$$U_{corr} = \sum_{i<j} u_2(r_{ij}) + \sum_{i<j,I} u_3(r_{ij}, r_{iI}, r_{jI}) + \cdots, \tag{17}$$

where $u_2(r_{ij})$ describes correlations between electrons i and j, and $u_3(r_{ij}, r_{iI}, r_{jI})$ describes the dominant 3-particle correlations of the type *electron-electron-nucleus* where I labels nuclei. To date the consideration of higher order correlations has been limited to that of Huang et al. [21]. The correlation functions u_2 and u_3 are further expanded in appropriate functions with expansion coefficients chosen to satisfy known analytic behavior of the exact wave function (typically the two-particle cusp conditions, satisfaction of which will keep the local energy bounded when two particles meet) and then optimized by VMC methods. A simple form of correlation function is the Pade–Jastrow (often referred to as the Jastrow factor) form [22]

$$u_2(r_{ij}) = \frac{a r_{ij}}{1 + b r_{ij}}. \tag{18}$$

Note that by including explicit correlation into the trial wave function, one is able to recover a large fraction of the correlation energy at the VMC level and significantly reduce the variance of the local energy by satisfying the electron–electron cusp condition.

In recent years, considerable effort has been invested in improvements of the antisymmetric function, Ψ_A because it determines the fermion nodes and therefore controls the fixed-node bias. The simplest antisymmetric wave function is a Slater determinant of spin orbitals. For QMC trial functions it has been shown [22] that this determinant can be factored into a product of spin-up and spin-down Slater determinants of orbitals,

$$\Psi_A = \begin{vmatrix} \phi_1^\alpha(r_1) & \cdots & \phi_1^\alpha(r_{n_\alpha}) \\ \vdots & \ddots & \vdots \\ \phi_{n_\alpha}^\alpha(r_1) & \cdots & \phi_{n_\alpha}^\alpha(r_{n_\alpha}) \end{vmatrix} \begin{vmatrix} \phi_1^\beta(r_1) & \cdots & \phi_1^\beta(r_{n_\beta}) \\ \vdots & \ddots & \vdots \\ \phi_{n_\beta}^\beta(r_1) & \cdots & \phi_{n_\beta}^\beta(r_{n_\beta}) \end{vmatrix} = D^\alpha D^\beta \tag{19}$$

or, more generally, a linear combination of such products,

$$\Psi_A = \sum_k c_k D_k^\alpha D_k^\beta. \tag{20}$$

The single determinant product multiplied by a Jastrow factor is often called a Slater–Jastrow wave function. Orbitals from various methods have been tested and utilized in such wave functions. Most popular have been HF and post-HF orbitals, such as those from

MCSCF and CI approaches. Orbitals from DFT have also been employed, in particular, a number of generalized gradient and hybrid functionals have been explored [20,23,24]. In addition, there has been some use of orbitals generated from Moeller–Plesset perturbation theory as well as direct optimization of orbitals together with other variational parameters, as will be mentioned below.

More recently, pair orbitals (geminals) have been introduced into QMC. This direction was pioneered in Sorella's group [25,26] with an antisymmetrized product of pair orbital that is known in condensed matter physics as the Bardeen–Cooper–Schrieffer (BCS) wave function, given by:

$$\Psi_A = \Psi_{BCS} = \det|\phi_v(r_i, r_j)|. \tag{21}$$

Here ϕ_v is a singlet pair orbital for a system of total spin zero. Although the form can be generalized to include spin-polarized states, for the fully spin-polarized state the wave function is uncorrelated as in HF. A more general form has been employed by Bajdich and coworkers [27,28],

$$\Psi_A = \mathrm{pf}[\phi(r_i, \sigma_i : r_j, \sigma_j)], \tag{22}$$

who introduced the use of a pfaffian(pf) matrix [27] of pair spin-geminals. The details of pfaffians are given elsewhere [27], however with assignment of electron spins, one can write the trial function as a pfaffian with pair orbitals/geminals with singlet and triplet coupling as well as orbitals for the unpaired electrons and thus describe correlation of any spin state.

For ease of computation, it is important that pfaffians can be evaluated by algorithms analogous to Gaussian elimination for determinants and have the same computational scaling in the number of particles. This approach has proved to be quite successful, and a single pfaffian has been found to lead to systematically improved results for the correlation energy recovered as has been confirmed on first-row atoms and molecules composed of such atoms [27]. Further improvements include expansions in pfaffians, which are much more compact than expansions in determinants, typically decreasing the number of terms by an order of magnitude while recovering 98–99% of the correlation energy for first-row systems [27].

Trial wave functions constructed following the transcorrelated form of Boys and Handy [16,17] have been used in VMC calculations with good recovery of correlation energy using the simple Slater–Jastrow trial function form [29]. Use of the simple Jastrow form in DMC calculations yielded results similar to those obtained with other single determinant trial functions [30]. It is anticipated that improved results might be possible using improved correlation functions of the type given by Eq. (17).

2.3.2. Trial wave function optimization

Optimization of trial wave functions in QMC is a complex and challenging task due to the overall nonlinearity of optimization and stochastic integral evaluation. Any optimization algorithm must deal with multiple issues of the statistical 'noise' of the quantities being optimized (typically the local energy or its variance), potential linear dependencies in the parameters, since they often constitute an over complete set, and the problems of local minima. Many of these problems have been effectively resolved in recent years and reportedly hundreds parameters can be optimized with good efficiency [31–33]. These developments have enabled the concurrent optimization of Jastrow parameters, determinant expansion coefficients, and one-particle orbitals for the C_2 molecule leading to an accuracy of better than 0.1eV for the atomization energy, effectively, reaching the experimental uncertainties. Very recently, thousands of parameters have been effectively optimized in simulations of liquid hydrogen [34].

The advantage of trial function optimization is exemplified in Fig. 2 taken from a study by Toulouse et al. [35] who compared

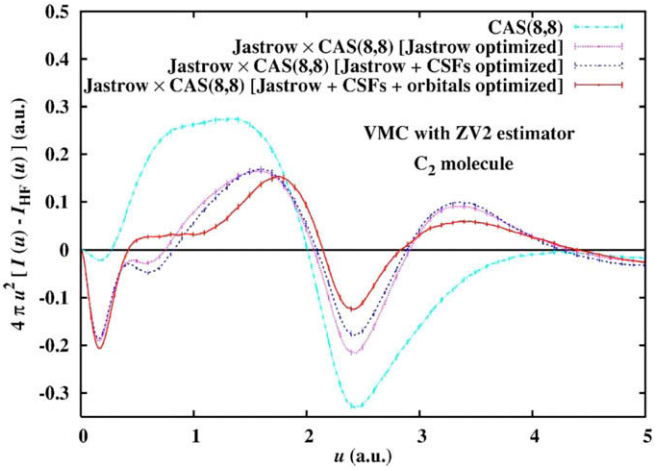

Fig. 2. Correlation part of the radial position intracule density $4\pi u^2[I(u) - I_{HF}(u)]$ as a function of the electron–electron distance u for the C_2 molecule, where I(u) has been calculated in VMC using the ZV2 improved estimator [with $\xi = 2\sqrt{2\mathbf{I}} \approx 1.83$ (Ref. [36])] with a MCSCF CAS (8,8) wave function and a series of Jastrow x CAS (8,8) wave functions with different levels of optimization. See Ref. [35] for notation.

the correlation part of the radial position intracule density for C_2 obtained using trial function optimized at various levels. Significant differences are found among the curves.

2.3.3. Evaluation of the trial function: approach to linear scaling

One of the most computationally intensive steps in the QMC algorithm is trial function evaluation, and specifically that of the Slater determinant. In general, the number of operations needed to evaluate the determinant, and hence the energy at each point of a QMC simulation, increases as N^3 where N is the rank of the determinant. For large systems the determinant becomes increasingly sparse because for gapped systems the correlation between localized electrons diminishes exponentially with distance [37].

In various implementations, a number of steps have been taken in order to obtain near-linear scaling [9–11]. In particular, wave function evaluation in the QMC code Zori follows the procedure of Aspuru-Guzik et al. [11] in which a sparse representation of the Slater matrix is used leading to evaluation of only the non-zero elements. This approach, combined with the use of localized orbitals in a Slater-type orbital basis set, significantly extends the size of molecule that can be treated with the QMC method – in this case the largest system contained over 300 electrons [38]. Tests confirm that this approach leads to linear scaling of Slater determinant evaluation with system size [11] and the calculation of excitation energies as N^2.

2.4. Pseudopotentials and effective core potentials

Pseudopotentials or effective core potentials (ECPs) are important for increasing efficiency of calculations for heavier atoms. As shown previously, the cost of calculations grows proportionally to $Z^{5.5-6.5}$ where Z is the atomic number [39,40]. Clearly, such Z dependence makes calculations of heavy-atom systems computationally demanding and inefficient with most of the computer time used for sampling large energy fluctuations in the core region, which typically has relatively little effect on chemical processes involving valence electrons. Despite this shortcoming, all-electron calculations have been carried out for systems containing atoms as large as Xe [4]. When the important chemistry and physics occurs in the valence space, it is often convenient to replace the core electrons with accurate ECPs suitable for QMC. The construction of such ECPs is therefore of prime importance, and often electrons

occupying the shell below the valence electrons are included in the valence space to take into account 'core polarization' effects, e.g., the 3s and 3p electrons would be included in the valence shell for the 3d-transition metals. The ability of QMC to incorporate ECPs has led to further ECP development including forms with smooth and bounded behavior at the nucleus [15,41–43].

Evaluation of ECPs in the VMC method is straightforward, however, in DMC and other exact QMC methods, the use of ECPs is more difficult. The ECP is in the form of a non-local integral operator, hence the value of the ECP at a single point depends on the entire wave function. In DMC the wave function is unknown, and so one must evaluate the ECP using Ψ_T rather than Φ_0, which leads to the so-called 'localization approximation' [40,44,45]. This approximation has enabled a number of important calculations that demonstrated that for accurate trial functions the bias is rather small (proportional to the square of the trial function error). A less desirable property of the localization approximation is that the resulting fixed-node energy is not an upper bound to the exact energy, and could introduce large energy fluctuations if the trial function is not sufficiently accurate. Based on QMC lattice model developments, ten Haaf and coworkers [46] showed how to construct an upper bound with the use of ECPs. The latter approach has been implemented in DMC [47] and resulted in reduced local energy fluctuations and increased stability of calculations.

2.5. Excited states

There is no difficulty in carrying out QMC calculations of excited states that are the lowest state of a given symmetry. One simply requires a trial wave function of the appropriate symmetry. Excited states of the same symmetry as a lower state are more difficult, in principle, owing to the absence of a theorem that insures that the calculation evolves to the appropriate excited state. Using a MCSCF trial function, an early calculation of the E state of H_2 confirmed the capability of the DMC method to calculate accurately the energy of an excited state of the same symmetry as a lower state which, in this case, was the ground state [19].

Challenging calculations of excited states for small hydrocarbon system have been carried out by Schautz and Filippi [48]. The difficulty comes from the fact that these systems exhibit a number of excited states that have nearly the same energy and are sensitive to the treatment of electron correlation. Using careful optimization of the variational trial functions used as importance functions for both ground and excited states, the authors were able to identify the correct excitations within the given symmetry types and to compute accurate relative differences.

2.6. Computation of properties other than the energy: moments, forces, equilibrium geometries, transition states

Calculations of properties that do not commute with Hamiltonian are more difficult to carry out with the fixed-node DMC method because the $\Psi_T\Phi_0$ distribution directly encountered is the mixed distribution and not the pure fixed-node solution. The calculation of pure expectation values requires sampling from the pure distribution which has been addressed by Barnett et al. [49,50] in studies of QMC expectation values of moments, by Rothstein et al. for differential operators [51] and relativistic corrections [52], and by Assaraf and Caffarel [53]. All 'pure' methods require the computation of weighting factors (either explicitly or by random walks) that correct for the mixed distribution. This adds significant computational effort beyond that required for the energy, and increases the variance of the computed property.

A second difficulty in computing properties other than the energy is that the associated estimators can have substantially larger fluctuations. Although importance sampling can reduce the variance of the local energy to zero for the exact trial function, this zero-variance principle does not hold for other properties such as, for example, the dipole moment operator. The magnitude of the variance is particularly significant for calculations of forces because the estimators involve derivatives of the total energy.

Various aspects of these complications have been tackled in recent years. As recently suggested, the variance issue can be addressed by modifying the estimator so that the fluctuations decrease significantly without biasing the resulting estimate [54].

An approach for avoiding the mixed estimator has been introduced by Moroni and Baroni [55] called reptation Monte Carlo. The method eliminates the DMC branching step and enables one to compute pure estimators using forward walking (or, more precisely, backward averaging) without the use of weights. To date the method has not been efficient for large systems, however, recent developments indicate that the method can be modified to remove this shortcoming [56]; see also Ref. [57].

Another approach that has yielded very good results is the phaseless auxiliary field quantum Mont Carlo (AFQMC) method [58]. In the usual AFQMC development, two-body interactions require auxiliary fields that are complex. As a result, MC averaging over auxiliary field configurations becomes integration over complex variables in many dimensions that leads to a phase problem that seemingly defeats the algebraic scaling of Monte Carlo and results in exponential scaling. This complication is analogous to but potentially more severe than the sign problem with real auxiliary fields or in real-space methods. In Zhang's approach, the sign problem in the complex plane is eliminated by projection onto the real axis that introduces an approximation analogous to the fixed-node approximation of the DMC method. The AFQMC approach makes possible the use of any one-particle basis and projects out the ground state by random walks in the space of Slater determinants. Less desirable features of this method are that the energy is not variational, and the amount of correlation energy recovered is limited by the size of the basis. Nevertheless, excellent results have been obtained with the method using a plane-wave basis and nonlocal pseudopotentials [59,60].

2.7. Beyond the fixed-node approximation

Exciting progress has been achieved in understanding the fundamental approximation of the DMC method, namely, the fixed-node bias. In particular, a conjecture by Ceperley [39] that the fermion node hypersurface divides the space of electron configurations into the minimal number of two domains for non-degenerate ground states has been explicitly demonstrated for a range of non-interacting systems and for important trial functions such as those based on pair functions in BCS and pfaffian forms. This work shows that the topologies of the nodal surfaces are almost always rather simple except for selected cases of quantum phase transitions and large-scale/infinite degeneracies or nonlocal interactions. This research has led to further investigations of shapes of nodal surfaces that are important for minimization of fixed-node errors using, for example, multi-pfaffian expansions [27,28]. This line of research has also opened a new direction that introduces concepts of topology and quantum geometry into electronic structure theory. Although much needs to be done, further research based on well-established ideas of field theory and quantum statistical mechanics is anticipated to influence both fundamental understanding of quantum systems and practical applications.

2.8. Coupling of QMC and molecular dynamics (MD) approaches

The first attempt to combine the strength of QMC with *ab intio* MD methods was reported by Grossman and Mitas [13]. This effort was based on efficient calculations of DMC energies along the nu-

clear trajectories generated by the *ab initio* DFT/MD method. The key gain was obtained by updating the walker distribution and DMC trial wave function along the nuclear paths. Nuclei in *ab initio* MD require very small time steps of order 0.001–0.0001 a.u., which is sufficient to enable the electronic walker distribution to relax in a few DMC steps. The latter are typically one to two orders of magnitude larger (0.1–0.01 a.u.). The authors found that about three DMC steps are enough to update the wave function for each step in nuclear position and that the QMC part of the calculation increased the overall computation by only a factor of two. Further, they found that although the detailed wave function information at any given step is determined by the walker distribution so that the error bars are significant at any single point in the MD simulation, over the period of the entire MD run, they were able to obtain thermodynamic averages with very small error bars. One of the key results was an estimation of the heat of water evaporation, a dynamical and finite temperature quantity, was found to be 9.1(4) kcal/mol, in excellent agreement with the experimental value of 9.9 kcal/mol (the DFT estimate is too small by about 30%). Very recently, Attaccalite and Sorella [34] carried out QMC/MD calculations with QMC forces for liquid hydrogen and evaluated its properties under various thermodynamic conditions.

2.9. Weak interactions

DMC studies of weakly bound molecules have established the capability of DMC to yield highly accurate interaction energies [61,3]. It was shown that DMC does not suffer from basis set superposition error owing to the convergence of monomer(s) with basis set, unlike other ab initio post-Hartree–Fock methods. For large systems, however, it was found that special attention must be paid to the ability of the atomic orbital basis set to describe the asymptotic behavior of the wave function to avoid sampling errors. Accurate results were reported for C_2, benzene and benzene dimer – one *T* shaped and the other displaced parallel to the first [62].

3. Applications

Following is a selected list of calculations with brief comments on types of DMC calculations that have been carried out to date. The list is biased towards calculations of the energy, for which DMC has been found to yield highly accurate results, although findings regarding other properties are also given.

3.1. Molecular systems involving first-row atoms

3.1.1. C_2H_4

A further validation of the DMC method for small molecules was recently reported in the form of the singlet-triplet splitting in ethylene. The property was computed using a large basis set with the CCSD(T) method and compared with the result of a DMC calculation with a Slater–Jastrow trial function. Excellent agreement between the computational methods was obtained; [63] see Table 1. The discrepancies with experiment are unexplained.

3.1.2. O_4

The weakly bound O_4 species has relevance for atmospheric processes. A recent DMC study has addressed the difficulties in describing the passage from a singlet O_4 reactant to two ground state O_2 triplet products [65]. The authors carefully addressed the issue of accurate differences of total energies for barriers and other properties. In this study, the exceptional step was taken of varying the multi-reference character of the nodes that made possible very high accuracy for energy differences.

3.1.3. Free base porphyrin

Accurate DMC calculations of allowed and non-allowed transitions in porphyrin have been reported [66]. The vertical transition between the ground state singlet and the second excited state singlet as well as the adiabatic transition between the ground state and the lowest triplet state were computed for this 162-electron system. The DMC results were found to be in excellent agreement with experiment. The results of this study including comparisons with other ab initio methods are given in Table 2 [65].

3.1.4. G1 benchmark study

A systematic study of DMC performance on the Gaussian-1 (G1) set of molecules [78] has been carried out by Grossman [79]. He used the simplest QMC single determinant Slater–Jastrow wave functions and found an absolute deviation of 2.9 kcal/mol. This finding placed the simplest form of DMC at roughly the same accuracy as the CCSD (T)/ aug-cc-pVQZ method. The largest error was found for P_2 molecule. This provided important systematic insight into the DMC performance at that time. It showed the great potential of DMC, but also pointed out that in difficult cases the simple Slater–Jastrow wave function might not be sufficient for desired accuracy.

Table 1
Summary of the calculated vertical and adiabatic singlet-triplet gap of ethylene (kcal/mol).[a]

Method	$\Delta E_{S\text{-}T}$ (vertical)[b] **2vert–1**	$\Delta E_{S\text{-}T,e}$ (adiabatic)[c] **2–1**	$\Delta E_{S\text{-}T}$ (adiabatic)[d] **2–1**
Present work			
CCSD(T)/aVDZ	103.8	65.6	62.4
CCSD(T)/aVTZ	103.7	67.7	64.5
CCSD(T)/aVQZ	103.9	68.4	65.2
CCSD(T)/aV5Z	104.0	68.6	65.4
CCSD(T)/CBS(1)	104.0	68.8	65.6
CCSD(T)/CBS(2)	104.1	68.8	65.6
TAE[e]			65.8
DMC[f]	103.5 ± 0.3		66.4 ± 0.3
Experimental	100.5[g]		58 ± 3[h]

[a] (U)CCSD (T)/a VTZ optimized geometries.
[b] Energy difference between **2vert** $^3B_{1u}$ and **1** ^1A_g states at the singlet **1** geometry.
[c] Energy difference between **2** $^3A_1$ and **1** $^1A_2$ without zero-point corrections.
[d] Energy difference **2** $^3A_1$ and **1** $^1A_2$ including zero-point corrections from Table 1 of Ref. [64].
[e] Negative difference between **2** $^3A_1$ and **1** $^1A_2$ based on the calculated (Q5) atomization energies given in Table 1 of Ref. [63].
[f] Diffusion Monte Carlo calculations taken from El Akramine et al. [63].
[g] Experimental result from Van Veen [91].
[h] Experimental estimate from Qi et al. [92].

Table 2
Excitation energies (eV) from the ground state to the **1** $^1B_{2u}$ and **1** $^3B_{2u}$ states of FBP. Empty slots indicate the absence of data.

Method	Vertical excitation (eV) **1** $^1B_{2u}$	Vertical excitation (eV) **1** $^3B_{2u}$	Adiabatic energy difference (eV) **1** $^3B_{2u}$
CIS[a]	2.66	1.23	
SAC-CI[b]	2.25		
CASPT2[c]	2.26	1.37	
TD-DFT[d]	2.39		
DFT-MRCI[e]	2.38		
MRSDCI[f]	2.40	1.65	
STEOM-CCSD(T)[g]	2.40	1.20	
DMC (this work)	2.45(8)		1.60(10)[k]
Experimental results			
Vapor phase[h]	2.42		
Supersonic jet[i]	2.46		
Frozen solvent[j]			1.58

[a] Ref. [67].
[b] Ref. [68].
[c] Ref. [69].
[d] Ref. [70].
[e] Ref. [71].
[f] Ref. [72].
[g] **1** $^1B_{2u}$: Ref. [73], **1** $^3B_{2u}$: Ref. [74].
[h] Ref. [75].
[i] Ref. [76].
[j] Ref. [77].
[k] Calculation performed at the minimum geometry of the B3LYP potential energy surface.

3.2. Transition metal systems

Significant progress has been achieved with DMC in the calculation of transition metal systems since the pioneering studies of Fe [80], $CuSi_n$ [81], and CO adsorption on a Cr(1 1 0) surface [82]. Recent developments include all-electron Green's function MC calculations of the 3d transition-metal atoms [83], and DMC calculations of the low-lying electronic states of Cu and its cation [84]. For the latter systems, the overall accuracy achieved with DMC for the nonrelativistic correlation energy (statistical fluctuations of about 1600 cm^{-1} and near cancelation of fixed-node errors) is good enough to reproduce the experimental spectrum when relativistic effects are included. These results illustrated that, despite the presence of large statistical fluctuations associated with core electrons, accurate all-electron DMC calculations for transition metals are presently feasible using extensive, but accessible computer resources.

An example of the accuracy of DMC for transition metal systems is further illustrated [72] in Fig. 3. The energy improvement for the Cu $^2S \rightarrow {}^2D$ transition is indicated from a Hartree–Fock approximation starting point extending to an all-electron DMC calculation that includes relativistic corrections.

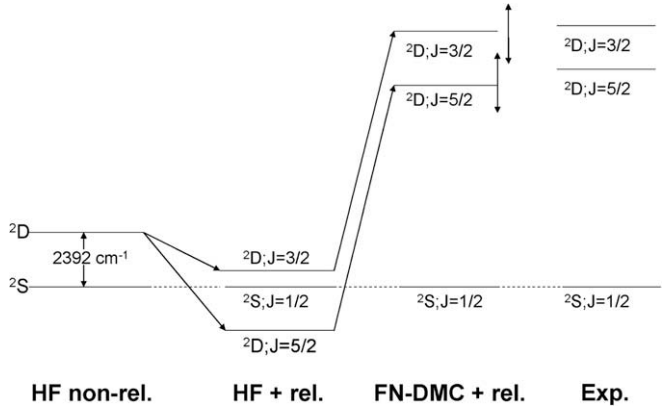

Fig. 3. Pictorial representation of the 2S → 2D transition with the various contributions considered. The SCF transition energy of 2392 cm^{-1} is indicated to set the scale. The vertical arrows in the FN-DMC+rel. column denote the statistical errors.

Other recent developments include calculations of binding energies, equilibrium bond lengths and dipole moments of the transition metal–oxygen molecules TiO [23] and MnO [24]. Calculations of energy-related quantities showed the strength of QMC quite clearly because with the simplest Slater–Jastrow trial functions results were reported on par with quite large CCSD(T) calculations *and* within a few percent of experiment or better. In addition, calculations involving bond-breaking are not much more complicated than other computations unlike the CCSD(T) method where special care has to be taken to obtain reliable results for such cases. Dipole moments showed somewhat larger discrepancies for CrO and MnO and called attention to the greater sensitivity of such calculations to the contribution of higher excitations than energy calculations [73]. The dipole moment provides a useful indicator of the missing components of a trial wave function and points out directions for improvements.

Very recently, large-scale QMC calculations have been carried out of FeO solid at high pressures for equilibrium properties including the equilibrium lattice constant, bulk modulus, and cohesive energy of 9.66(6) eV per FeO (experiment 9.7(1) eV per FeO). These properties were found to be in excellent agreement with experiment [85].

Some thoughts for the future

The current central challenges of QMC are focused on several basic problems. One is the fixed-node approximation, or, in a broader perspective, the fermion sign problem. The fixed-node method misses only 5–10% of the correlation energy and therefore captures enough many-body effects to predict significant quantities such as cohesive energies, barrier heights, optical gaps, and similar quantities to within a few percent of experiments. However, the missing correlation is nevertheless crucial for many subtle effects such as magnetic phenomena, differences between low-lying near degenerate states and macroscopic quantum phenomena such as superconductivity observed in, for example, certain transition metal oxides. The second issue is the development of methods for very large systems that bring their own set of problems such as necessity for more efficient and accurate representation of orbitals, more robust elimination of finite size errors for solids and surface calculations with periodic boundary conditions

and related tasks.The third challenge is the adaptation of QMC methods for large-scale parallelism offered by the upcoming class of petaflop and beyond machines. This requires rebuilding some of the core algorithms to provide more flexibility for exploiting multi-core processors and reorganization of calculations to enable use of tens of thousand processors on a routine basis.

Software packages

Some of the QMC methods are implemented in several existing codes and packages that are available for use by communities at large. We will mention the packages which are most familiar to us: CASINO [86], QMCPACK [87], QWALK [88], and CHAMP [89]. QMCPACK and QWALK are distributed under Open Source licenses.

Although not a software package, we mention here the novel approach for meeting the high computer demands of DMC by Korth et al. [90]. It is a distributed computational system that uses the power of ~38 000 PCs located all over the world. The system yields ~15 teraflops of sustained computing power.

Closing statement

In this review we have attempted to provide an overview of the QMC method for electronic structure with emphasis on the more accurate DMC variant of the method. The computation of energies and other properties are indicated. Recent developments are presented that shed light on the capability of the method for the computation of systems larger than those accessible by other ab initio methods.

Acknowledgements

W.A.L. was supported by the Director, Office of Science, Office of Basic Energy Sciences, Chemical Sciences Division of the US Department of Energy under Contract No. DE-AC03-76SF00098, the CREST Program of the US National Science Foundation, and by NSF CHE-0809969. L.M. is supported by NSF grants EAR-0530110 and DMR-0804549, and by the DOE 'Endstation' Grant DE-FG05-08OR23337, and some of L.M.'s projects mentioned in the paper have been carried out using INCITE and CNMS allocations at DOE ORNL computing facilities. L.M. also acknowledges support and hospitality of Aspen Center for Physics workshop during which some parts of this Letter were written.

References

[1] A. Aspuru-Guzik, W.A. Lester Jr., Quantum Monte Carlo for the solution of the Schroedinger equation for molecular systems, in: C. Le Bris (Ed.), Special Volume Computational Chemistry, in: P.G. Ciarlet (Ed.), Handbook of Numerical Analysis, Elsevier, 2003, p. 485.
[2] A. Aspuru-Guzik, W.A. Lester Jr., Adv. Quant. Chem. 49 (2005) 209.
[3] A. Luechow, J.B. Anderson, Ann. Rev. Phys. Chem. 51 (2000) 501.
[4] M.D. Towler, Phys. Stat. Sol. (b) 243 (2006) 2573.
[5] (a) See, for example S. Gandolfi, F. Pederiva, S. Fantoni, K.E. Schmidt, Phys. Rev. Lett. 99 (2007) 022507;
(b) J. Carlson, Nuc. Phys. A 787 (2007) 516.
[6] D. Shin, M.-C. Ho, J. Shumway, 2006. Available from: <arXiv:quant-ph/0611105v1>.
[7] A.B. McCoy, in: J.B. Anderson, S.M. Rothstein (Eds.), Proceedings of the Pacifichem Symposium on Advances in Quantum Monte Carlo, ACS Symposium Series, vol. 953, 2007, p. 55.
[8] J.B. Anderson, Quantum Monte Carlo Origins, Development, Applications, Oxford, 2007.
[9] A.J. Williamson, R.Q. Hood, J.C. Grossman, Phys. Rev. Lett. 87 (2001) 172301.
[10] S. Manten, A. Luchow, in: S.M. Rothstein, W.A. Lester Jr., S. Tanaka (Eds.), Quantum Monte Carlo Methods, Part II, World Scientific, Singapore, 2002, p. 30 (see also J. Chem. Phys. 11 (2003) 1307).
[11] A. Aspuru-Guzik, R. Salomon-Ferrer, B. Austin, W.A. Lester Jr., J. Comput. Chem. 26 (2005) 708;
A. Aspuru-Guzik et al., J. Comput. Chem. 26 (2005) 856.
[12] See section on 'Software Packages' at the end of the paper.
[13] J.C. Grossman, L. Mitas, Phys. Rev. Lett. 94 (2005) 056403.
[14] D. Bressanini, P.J. Reynolds, Adv. Chem. Phys. 105 (1999) 37.
[15] I. Ovcharenko, A. Aspuru-Guzik, W.A. Lester Jr., J. Chem. Phys. 114 (2001) 7790.
[16] S.F. Boys, N. Handy, Proc. Roy. Soc. London Ser. A 309 (1969) 209. 310 (1969) 43; 310 (1969) 63; 311 (1969) 309.
[17] K.E. Schmidt, J.W. Moskowitz, J. Chem. Phys. 93 (1990) 4172.
[18] J.B. Anderson, J. Chem. Phys. 65 (1976) 4121.
[19] R.M. Grimes, B.L. Hammond, P.J. Reynolds, W.A. Lester Jr., J. Chem. Phys. 84 (1986) 4749.
[20] See, for example, J.C. Grossman, W.A. Lester Jr., S.G. Louie, J. Am. Chem. Soc. 122 (2000) 705.
[21] C.-J. Huang, C.J. Umrigar, M.P. Nightingale, J. Chem. Phys. 107 (1997) 3007.
[22] P.J. Reynolds, D.M. Ceperley, B.J. Alder, W.A. Lester Jr., J. Chem. Phys. 77 (1982) 5593.
[23] L.K. Wagner, L. Mitas, Chem. Phys. Lett. 370 (2003) 412.
[24] L.K. Wagner, L. Mitas, J. Chem. Phys. 126 (2007) 034105.
[25] M. Casula, S. Sorella, J. Chem. Phys. 119 (2003) 6500.
[26] M. Casula, C. Attaccalite, S. Sorella, J. Chem. Phys. 121 (2004) 7110.
[27] M. Bajdich, L.K. Wagner, G. Drobny, L. Mitas, K.E. Schmidt, Phys. Rev. Lett. 96 (2006) 130201;
L. Mitas, Phys. Rev. Lett. 96 (2006) 240402.
[28] M. Bajdich, L. Mitas, L.K. Wagner, K.E. Schmidt, Phys. Rev. B 77 (2008) 115112.
[29] N. Umezawa, S. Tsuneyuki, T. Ohno, K. Shiraishi, T. Chikyow, J. Chem. Phys. 122 (2005) 224101;
N. Umezawa, S. Tsuneyuki, J. Chem. Phys. 119 (2003) 10015.
[30] R. Prasad, N. Umezawa, D. Domin, R. Salomon-Ferrer, W.A. Lester Jr., J. Chem. Phys. 126 (2007) 164109.
[31] C.J. Umrigar, J. Toulouse, C. Filippi, S. Sorella, R.G. Hennig, Phys. Rev. Lett. 98 (2007) 110201.
[32] C.J. Umrigar, C. Filippi, Phys. Rev. Lett. 94 (2005) 150201.
[33] X. Lin, H. Zhang, A.M. Rappe, J. Chem. Phys. 112 (2000) 2650.
[34] C. Attaccalite, S. Sorella, Phys. Rev. Lett. 100 (2008) 114501.
[35] J. Toulouse, R. Assaraf, C.J. Umrigar, J. Chem. Phys. 126 (2007) 244112.
[36] NIST Chemistry Webbook, NIST Standard Reference Database Number 69, June 2005 Release, <http://webbook.nist.gov/chemistry>.
[37] P. Maslen, C. Ochsenfeld, C. White, M. Lee, M. Head-Gordon, J. Phys. Chem. A 102 (1998) 2215.
[38] W.A. Lester Jr., R. Salomon-Ferrer, Theochem. 771 (2006) 51.
[39] D.M. Ceperley, J. Stat. Phys. 63 (1991) 1237.
[40] B.L. Hammond, P.J. Reynolds, W.A. Lester Jr., J. Chem. Phys. 87 (1987) 1130.
[41] C.W. Greef, W.A. Lester Jr., J. Chem. Phys. 109 (1998) 1607.
[42] Y. Lee, P.R. Kent, M.D. Towler, R.J. Needs, G. Rajagopal, Phys. Rev. B 62 (2000) 13347.
[43] M. Burkatzki, C. Filippi, M. Dolg, J. Chem. Phys. 126 (2007) 234105.
[44] M.M. Hurley, P.A. Christiansen, J. Chem. Phys. 86 (1987) 1069.
[45] L. Mitas, E.L. Shirley, D.M. Ceperley, J. Chem. Phys. 95 (1991) 3467.
[46] D.F. ten Haaf, H.J. van Bemmel, J.M. van Leeuwen, W. van Saarloos, D.M. Ceperley, Phys. Rev. B 51 (1995) 13039;
H.J. van Bemmel, D.F. ten Haaf, W. van Saarloos, J.M. van Leeuwen, G. An, Phys. Rev. Lett. 72 (1994) 2442.
[47] M. Casula, Phys. Rev. B 74 (2006) 161102.
[48] F. Schautz, C. Filippi, J. Chem. Phys. 120 (2004) 10931;
F. Schautz, C. Filippi, J. Chem. Phys. 121 (2004) 5836.
[49] R.N. Barnett, P.J. Reynolds, W.A. Lester Jr., J. Comput. Phys. 96 (1991) 258.
[50] R.N. Barnett, P.J. Reynolds, W.A. Lester Jr., J. Chem. Phys. 96 (1992) 2141.
[51] J. Vrbik, D.A. Legare, S.M. Rothstein, J. Chem. Phys. 92 (1990) 1221;
J. Vrbik, S.M. Rothstein, J. Chem. Phys. 96 (1992) 2071.
[52] J. Vrbik, M.F. DePasquale, S.M. Rothstein, J. Chem. Phys. 88 (1988) 3784.
[53] R. Assaraf, M. Caffarel, J. Chem. Phys. 113 (2000) 4028.
[54] R. Assaraf, M. Caffarel, J. Chem. Phys. 119 (2003) 10536.
[55] S. Baroni, S. Moroni, Phys. Rev. Lett. 82 (1999) 4745.
[56] S. Moroni, private communication.
[57] W.K. Yuen, T.J. Farrar, S.M. Rothstein, J. Phys. A: Math. Theor. 40 (2007) F639.
[58] S. Zhang, H. Krakauer, Phys. Rev. Lett. 90 (2003) 136401.
[59] M. Suewattana, W. Purwanto, S. Zhang, H. Krakauer, E.J. Walter, Phys. Rev. B 75 (2007) 245123.
[60] W.A. Al-Saidl, S. Zhang, H. Krakauer, J. Chem. Phys. 127 (2007) 14401.
[61] M. Mella, J.B. Anderson, J. Chem. Phys. 119 (2003) 8225.
[62] S. Sorella, M. Casula, D. Rocca, J. Chem. Phys. 127 (2007) 014105.
[63] O. El Akramine, A.C. Kollias, W.A. Lester Jr., J. Chem. Phys. 119 (2003) 1483.
[64] M.T. Nguyen, M.H. Matus, W.A. Lester Jr., D.A. Dixon, J. Phys. Chem. A 112 (2008) 2082.
[65] M. Caffarel, R. Hernandez-Lamoneda, A. Scemama, A. Ramırez-Solıs, Phys. Rev. Lett. 99 (2007) 153001.
[66] A. Aspuru-Guzik, O. El Akramine, J.C. Grossman, W.A. Lester Jr., J. Chem. Phys. 120 (2004) 3049.
[67] J.B. Foresman, M. Head-Gordon, J.A. Pople, M.J. Frisch, J. Phys. Chem. 96 (1992) 135.
[68] H. Nakatsuji, J. Hasegawa, M. Hada, J. Chem. Phys. 104 (1995) 2321.
[69] M. Merchan, E. Orti, B.O. Roos, Chem. Phys. Lett. 226 (1994) 27.
[70] D. Sundholm, Phys. Chem. Chem. Phys. 2 (2000) 2275.
[71] A.B.J. Parusel, S.J. Grimme, Porphyrins Phtalocyan. 5 (2001) 225.
[72] Y. Yamamoto, T. Noro, K. Ohno, Int. J. Quant. Chem. 42 (1992) 1563.
[73] S.R. Gwaltney, R.J. Bartlett, J. Chem. Phys. 108 (1998) 6790.
[74] M. Nooijen, R.J. Bartlett, J. Chem. Phys. 106 (1997) 6449.
[75] L. Edwards, D.H. Dolphin, J. Mol. Spectrosc. 38 (1971) 16.

[76] U. Even, J. Jortner, J. Chem. Phys. 77 (1982) 4391.
[77] M. Gouterman, G. Khalil, J. Mol. Spectrosc. 53 (1974) 88.
[78] J.A. Pople, M. Head-Gordon, D.J. Fox, K. Raghavachari, L.A. Curtiss, J. Chem. Phys. 90 (1989) 5622.
[79] J.C. Grossman, J. Chem. Phys. 117 (2002) 1434.
[80] L. Mitas, Phys. Rev. A 49 (1994) 4411.
[81] I.V. Ovcharenko, W.A. Lester Jr., C. Xiao, F. Hagelberg, J. Chem. Phys. 114 (2001) 9028.
[82] O. El Akramine, W.A. Lester Jr., X. Krokidis, C.A. Taft, T.C. Guimaraes, A.C. Pavao, R. Zhu, Mol. Phys. 101 (2003) 277.
[83] A. Sarsa, E. Buendia, F.J. Galvez, P. Maldonado, J. Phys. Chem. A 112 (2008) 2074.
[84] M. Caffarel, J.-P. Daudey, J.-L. Heully, A. Ramírez-Solís, J. Chem. Phys. 123 (2005) 094102.
[85] J. Kolorenc, L. Mitas, Phys. Rev. Lett. 101 (2008) 185502.
[86] R.J. Needs, M.D. Towler, N.D. Drummond, P.R.C. Kent, CASINO Version 1.8 User Manual University of Cambridge, Cambridge, 2005.
[87] <http://www.mcc.uiuc.edu/qmc/qmcpack/index.html>.
[88] L.K. Wagner, M. Bajdich, L. Mitas, J. Comput. Phys. 228 (2009) 3390. <http://www.qwalk.org>.
[89] <http://pages.physics.cornell.edu/~cyrus/champ.html>.
[90] M. Korth, A. Luechow, S. Grimme, J. Phys. Chem. A 112 (2008) 2104.
[91] E.H. Van Veen, Chem. Phys. Lett. 41 (1976) 540. (4.36 eV).
[92] F. Qi et al., J. Chem. Phys. 112 (2000) 10707.

Glossary

VMC: variational Monte Carlo
DMC: diffusion Monte Carlo
AFQMC: auxiliary field quantum Monte Carlo
BCS: Bardeen–Cooper–Schrieffer
MCSCF: multi-configuration self-consistent field
CI: configuration interaction
DFT: density functional theory
fixed-node approximation: imposition of the nodes of a given approximate trial function as the nodes of the exact wave function
wave function node: coordinate value at which the wave function vanishes; a subset of configurations with zero wave function value
pfaffian: antisymmetric sum of pairwise distinct permutations, generalization of the determinant; wave function formed by antisymmetrization of a pair-orbital product

William A. Lester Jr. is Professor of Chemistry, University of California, Berkeley and Faculty Senior Scientist, Lawrence Berkeley National Laboratory. He holds B.S., M.S., and Ph.D. degrees, all in chemistry. He has held professional appointments at the University of Wisconsin, Madison, the IBM Research Division, and the NSF. He has published numerous scientific articles, a book on QMC, and is editor or co-editor of four other volumes on QMC. He is a Fellow of he APS, the American Association for the Advancement of Science, the California Academy of Sciences, and a member of the International Academy of Quantum Molecular Science.

Dr. Lubos Mitas obtained his undergraduate degree in physics at the Slovak Technical University, Bratislava, Slovakia in 1983. He joined the Institute of Physics, Slovak Academy of Sciences in 1984 and obtained his PhD degree there in 1989. In 1990–1999 he worked with R.M. Martin and D.M. Ceperley at University of Illinois at Urbana-Champaign as a Postdoctoral Research Associate, NSF Postdoctoral Fellow, and Research Scientist. In 2000, he was appointed Assistant Professor in the Department of Physics at North Carolina State University, Raleigh, in 2003 Associate Professor, and in 2006 Full Professor. His research includes methods for simulations of many-body quantum and classical systems, electron correlation effects in molecules, nanostructures and solids and problems in mathematical physics such as topological properties of many-body wave functions. For further information, see http://altair.physics.ncsu.edu/.

Brian Hammond is part of Microsoft's high performance computing (HPC) team focusing on the life sciences and academic research. Brian earned a B.S. degree at Harvey Mudd College, his Ph.D. in computational chemistry at the University of California, Berkeley, and is co-author of the seminal book 'Quantum Monte Carlo Methods in ab initio Quantum Chemistry' (World Scientific). Since then he has worked for many of the industry's leading IT companies: IBM, Fujitsu, Cray, SGI and Sun. Brian is now working with the Microsoft team to bring HPC to an even wider audience, and to help users and developers become more productive as they take on their grand challenge problems.